Combination of two fat saturation pulses improves detectability of glucose signals in carbon-13 MR spectroscopy

By Moyoko TOMIYASU,[*1] Tsuyoshi MATSUDA,[*2] James TROPP,[*3] Toshiro INUBUSHI[*4] and Toshiharu NAKAI[*5,†]

(Communicated by Masanori OTSUKA, M.J.A.)

Abstract: In order to improve the fat suppression performance of *in vivo* ^{13}C-MRS operating at 3.0 Tesla, a phantom model study was conducted using a combination of two fat suppression techniques; a set of pulses for frequency (chemical shift) selective suppression (CHESS), and spatial saturation (SAT). By optimizing the slab thickness for SAT and the irradiation bandwidth for CHESS, the signals of the $-^{13}CH_3$ peak at 49 ppm and the $-^{13}CH_2-$ peak at 26 ppm simulating fat components were suppressed to 5% and 19%, respectively. Combination of these two fat suppression pulses achieved a 53% increase of the height ratio of the glucose C1β peak compared with the sum of all other peaks, indicating better sensitivity for glucose signal detection. This method will be applicable for *in vivo* ^{13}C-MRS by additional adjustment with the *in vivo* relaxation times of the metabolites.

Keywords: ^{13}C, MRS, CHESS, spatial saturation (SAT), fat suppression, glucose

Introduction

In vivo carbon-13 magnetic resonance spectroscopy (^{13}C-MRS) is expected to be potentially useful for clinical application, especially to monitor glucose metabolites in the tissues or organs. One such application of glucose monitoring using ^{13}C-MRS is to improve early detection of metabolic change in the liver or muscle and to evaluate post-therapeutic changes in diabetic patients.[1)–4)] Higher static magnetic field (B0) of the MR system is advantageous to detect subtle signals originating from the compounds distributed *in vivo*, however, heating due to the radio frequency (RF) pulse for decoupling, which is applied to extract each peak of the ^{13}C spectra, increases depending on the B0 strength. To minimize heating and avoid tissue damage, surface coils are employed to detect local signals; however, this method does not permit the supression of the lipid signal. In ^{13}C MRS measurements without stable isotope labeling, natural ^{13}C signals originating from the subcutaneous fat tissue and the visceral lipid signals included in the organ tissue of interest are much larger than those from the target metabolites.

A three-dimensional localization technique such as ISIS[5)] or outer volume suppression (OVS), which uses six hyperbolic secant pulses,[6),7)] has been proposed to remove the contamination of ^{13}C lipid signals attributed to extra-cerebral fat tissue.[8)] The disadvantage of these techniques is the inability to suppress the signals from visceral fat. The following two methods have been employed to suppress lipid signals in ^{1}H MRS, 1) frequency (chemical shift) selective suppression pulses (CHESS)[9)] based on the frequency difference due to the chemical shift, such as those between a proton of water and that of fat, and 2) spatial saturation (SAT) pulses to reduce all signals included in the slab located on the subcutaneous fat layer. In this study, we performed a phantom model study to validate these two types of lipid suppression pulses and their combination for ^{13}C MRS on a clinical 3.0 Tesla (T) MR scanner. The

[*1] Research Program for Carbon Ion Therapy and Diagnostic Imaging, Research Center for Charged Particle Therapy, National Institute of Radiological Sciences, Chiba, Japan.
[*2] Applied Science Laboratory Asia Pacific, GE Healthcare Japan Corporation, Tokyo, Japan.
[*3] Global Applied Sciences Lab, GE Healthcare Corporation, CA, U.S.A.
[*4] Biomedical MR Science Center, Shiga University of Medical Science, Shiga, Japan.
[*5] Neuroimaging and Informatics Lab, Division of Gerontechnology, National Center for Geriatrics and Gerontology, Aichi, Japan.
[†] Correspondence should be addressed: Toshiharu Nakai, PhD, Niinf NCGG, 36-3 Gengo, Morioka-cho, Ohbu, Aichi 474-8522, Japan (e-mail: toshi@ncgg.go.jp).

doi: 10.2183/pjab.87.425

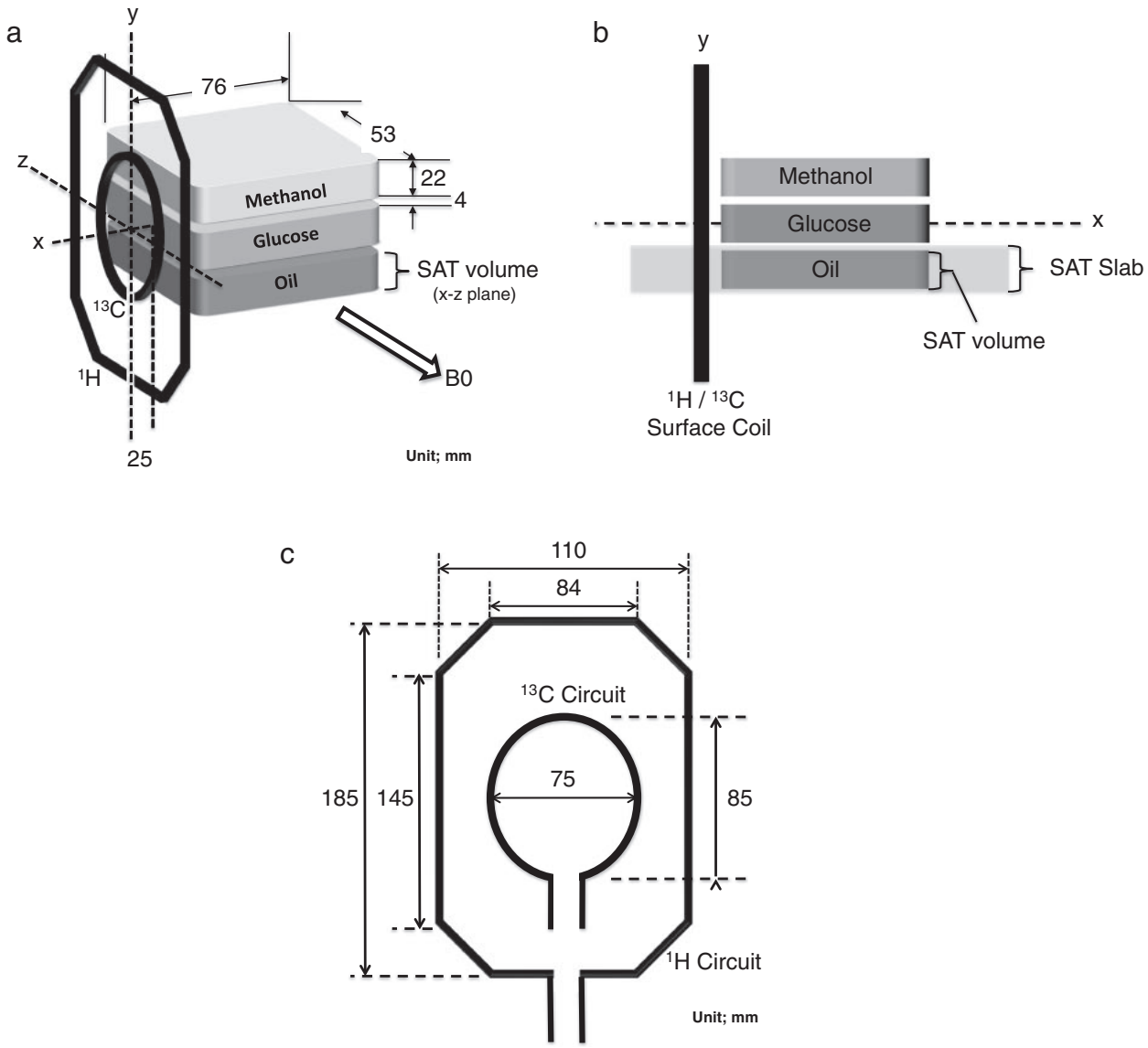

Fig. 1. Design of a phantom study using a pair coil set for ^{1}H and ^{13}C. 1a: The three phantom components were stacked and placed beside the coil surface in the axial view. The surface coil was placed parallel to the B0 direction (in y–z plane). SAT pulse was applied to the slab in x–z plane (1b) covering the oil component ('SAT volume' corresponding to the plastic case at the bottom). Using a proton MR image of the phantom, the spatial location of 'SAT volume' was automatically configured. CHESS pulse was applied to and ^{13}C spectra were obtained from the whole volume including the three components. 1c: Circuit design of the surface coil pair. The inner oval coil was adjusted for ^{13}C resonance and the outer octagon circuit for ^{1}H. These two circuits are electrically independent.

optimal parameters to achieve lipid suppression *in vivo* were investigated.

Materials and methods

MR systems for the ^{13}C MRS experiments. All MRI and MRS experiments were performed with a 3.0 T clinical MR system equipped with a second channel transmit/receive system (Signa VH/i 3.0 T; GE Healthcare, Milwaukee, WI). Proton and ^{13}C MR data were obtained using a custom-made transmit/receive surface coil unit (GE Healthcare, Fig. 1) with external dimensions of $195 \times 130\,\mathrm{mm}^2$. The resonator circuits were designed to be independent of each other. The ellipsoid of the ^{13}C resonator (32.16 MHz) was $85 \times 75\,\mathrm{mm}^2$, and that of the proton resonator (127.89 MHz) was $185 \times 110\,\mathrm{mm}^2$ (Fig. 1c). The ^{13}C resonator was located concentrically inside of the proton resonator.

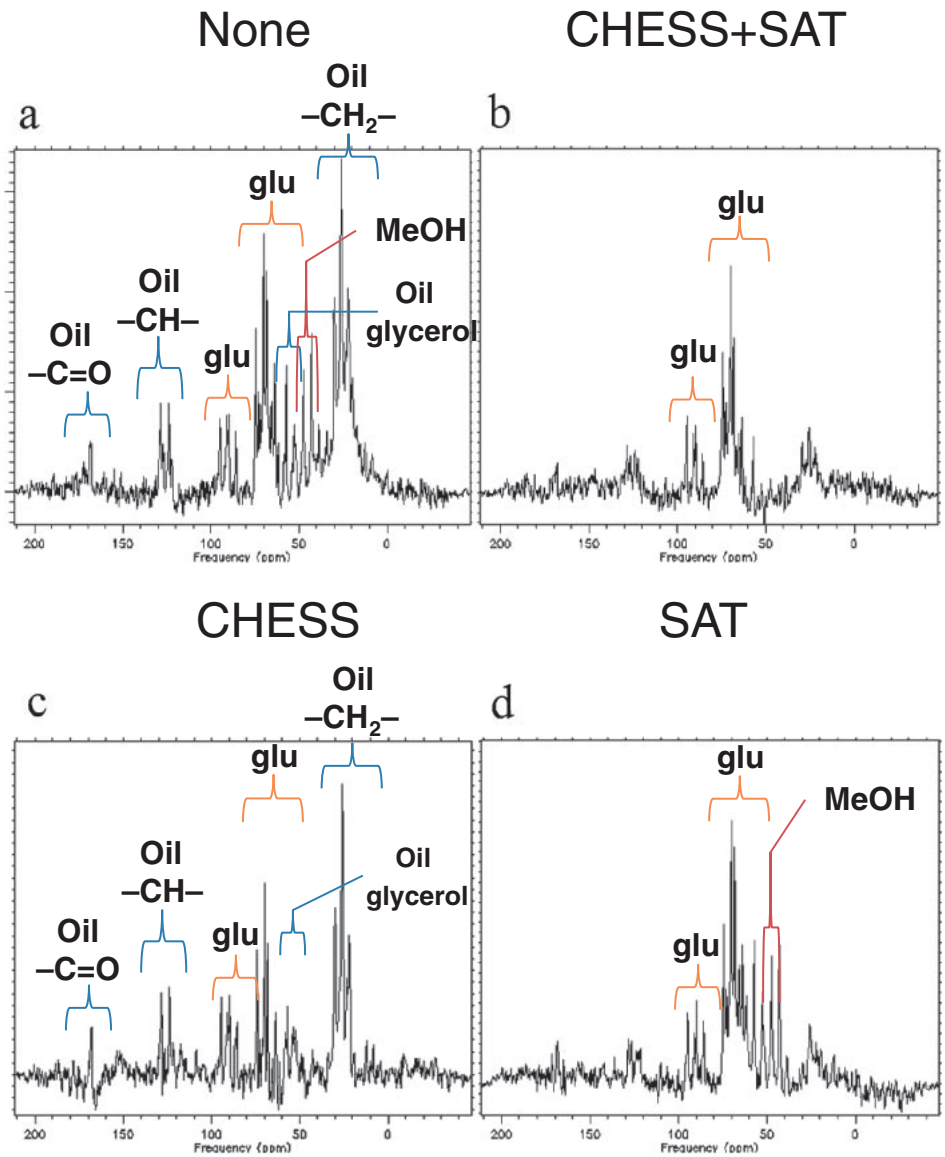

Fig. 2. The ^{13}C MR spectra of the phantom. The ^{13}C MR spectra of the methanol, glucose and oil phantoms. The scale of vertical axes is arbitrary unit. Signals from methanol and lipid were observed in a wide range of chemical shift without CHESS and SAT pulses (2a). For example, spectral quantification analysis using SA/GE indicated that signal residue of the carbonyl carbon at 168 ppm was 40% with CHESS and SAT pulses (2b). The methanol signals around 49 ppm were suppressed with the CHESS pulse (2c). The lipid signals at various frequencies (26 (CH_2), 128 (CH) and 168 ppm (C=O)) were well suppressed by the SAT pulse (2d).

Phantom preparation. A phantom was designed to include three components, 99.9% methanol (Aldrich Chemical, Milwaukee, WI), a mixture of canola and soybean oil (Nisshin Oil Group, Tokyo, Japan) and non-enriched D(+) glucose–water solution (3.2 mol/kg, Nacalai Tesque, Kyoto, Japan). Glucose rather than glycogen was chosen as the target metabolite in this study for better quantification of signal detection. The oil signals imitated the ^{13}C spectra originating from subcutaneous fat, and those of methanol partially simulated visceral fat in an organ. Methanol was employed to simulate the $-CH_3$ peaks of lipid components, since they are located within a similar chemical shift range to the lipid peaks and can be distinguished from other peaks originating from the mixture oil compounds. In order to assess the efficacy of the SAT pulses on each component, the three components were spatially separated in three plastic cases (Fig. 1). The internal dimension of each case was $76 \times 53 \times 22\,mm^3$.

Pulse sequence for suppressing ^{13}C signals. CHESS and SAT pulses for ^{13}C-MRS were combined as follows:

CHESS – SAT – ^{13}C hard pulse
– MR signal acquisition

A single excitation pulse was used for both CHESS and SAT, and the duration times were 50 ms and 10 ms, respectively. The hard pulse duration time for ^{13}C was 250 µs. Selective excitation pulses for CHESS and SAT were designed with the Shinnar–Le Roux algorithm,[10),11)] which is based on a discrete approximation to the spin domain version of the Bloch equation. The excitation pulses equivalent to the *sinc* shape were generated by using a series of small hard pulses modulated to represent the waveform amplitude. The center frequency, pulse strength and bandwidth were varied to identify the best condition. The slab volume to be suppressed by applying the SAT pulse with a resonance frequency of ^{13}C was determined by ^{1}H MR imaging. The resonance frequency of ^{13}C (32.16 MHz) at 3.0 T was automatically adjusted depending on that of ^{1}H (127.89 MHz) by a pulse sequence program equipped with a second channel system. The irradiation bandwidth of the RF pulse for SAT slice selection was fixed at 6000 Hz, which corresponded to 5.6 gauss for ^{13}C at 3.0 T. The field gradient strength, which was inversely proportional to SAT slice thickness, was changed to determine the slice thickness:

(slab thickness (cm))
× (gradient strength (gauss/cm))
= 5.6 gauss

In this study, the gradient strength was configured to be 2.2 gauss/cm so that the SAT slab covers 25.2 mm thickness depending on the height of the plastic case.

^{13}C MR experiments with two suppression sequences. The phantom consisting of the three components was placed close to the coil surface, as shown in Fig. 1. Before the ^{13}C MRS experiment, the first-order shim coil currents were automatically adjusted by a proton phase image. The parameters for ^{13}C MRS were TR 500 ms, observation bandwidth 8 kHz, sampling points 512 and number of data acquisitions 512. Twenty-four dummy scans were performed to achieve a steady state of magnetization. A CHESS pulse was used to suppress multiple signals of methanol $-^{13}CH_3$, with a bandwidth of 400 Hz, flip angle of 150° and center frequency of 49 ppm. The flip angle was calculated by the total signal intensity received by the surface coil. To apply the SAT pulse over the slab including the oil component case with ^{13}C resonance frequencies, a proton MR image was used for localization, and the center frequency was changed from the proton resonance to that of ^{13}C at 82 ppm automatically (Fig. 1). The RF power to achieve maximum fat suppression was obtained for each of SAT and CHESS.

Spectral analysis to quantify each ^{13}C peak was performed using the SA/GE software package (GE Healthcare) on a workstation (IRIX O_2, Silicon Graphics, Mountain View, CA). The averaged FIDs were processed with a 10 Hz exponential window function, zero-filled to double the sampling points, fast Fourier transformed, manually phase corrected, and cubic spline baseline correction was applied.

Results

Figure 2 shows the ^{13}C MR spectra obtained from the phantom with or without CHESS and SAT sequences. Table 1 shows the relative heights of each peak with both and without either sequence. Signal assignments of the oil were based on references.[12)–15)] The reduction rate of 7 out of 8 peaks with both suppression pulses showed good agreement with the sum of separate SAT/CHESS pulses. With the combination of SAT and CHESS pulses, the residual rate of the oil carbonyl carbon peak (C=O, 168 ppm) was 40% of that without fat suppression (60% reduction), however, it was 83% (only 17% reduction) with SAT alone. The height percentages of the glucose C1β peak compared with the sum of all other peaks without and with the two suppression sequences were 21.8% and 33.4%, respectively, leading to a 53% increase in the relative scale of the glucose signal. With the CHESS pulse, the methanol $-CH_3$ peaks centering around 49 ppm were suppressed to the residual rate of 13%. With additional removal of non-methanol $-CH_3$ peaks by SAT pulse, the total signal was just 5% (95% reduction). Simultaneously, CHESS suppressed the signals originating from glucose C6 and/or glycerol (58 ppm) to 56%. Lipid signals from the oil component at various frequencies (26, 128 and 168 ppm) were decreased with SAT, especially reducing the $-CH_2-$ signals (26 ppm) to 18% (reduction rate of 82%). Glucose signals of C3 and C5 (70 ppm) might have been reduced by the CHESS pulse, since the excitation profile of CHESS was not strictly rectangular. Glucose signals ranging over 70 to 95 ppm were not affected by either of the fat suppression pulses.

Table 1. Relative signal intensities (residual rate) of the ^{13}C spectra

Phantom component	Glucose	Glucose	Glucose	Glucose/Oil	Methanol	Oil	Oil	Oil
Carbon group	C1α	C1β	C3/C5	C6/glycerol	CH_3	CH_2	CH	C=O
Chemical shifts (ppm)	90	96	70	58	49	26	128	168
CHESS and SAT (%)	100	86	87	44	5	19	53	40
CHESS (%)	96	100	77	56	13	90	95	98
SAT (%)	100	100	100	100	87	18	49	83

Each peak was obtained by applying Fourier transformation to the average of 1024 FIDs. The baseline (100%) was obtained by using the highest peak induced by J couplings without the two fat suppression pulse sequences. The chemical shifts (ppm) were observed in this experiment and their assignments were based on the references[12),13),14),15)] (see Fig. 2).

Discussion and conclusions

It was demonstrated that ^{13}C fat signals could be most effectively suppressed *in vitro* by the combination of SAT and CHESS pulses, which reduce the signals of both subcutaneous and visceral fat. The optimum TR value for the best fat suppression condition and better detection of the target metabolite depends on their relaxation times. Since longer TR increases the total scan time, shorter TR will be practical for clinical usage, however, shorter TR reduces the detectability of glucose or low molecular weight metabolites with longer T1 than those of fat components. It was reported that *in vivo* and *in vitro* T_1 relaxation times of [1-^{13}C] liver glycogen were 150–170 ms[16),17)] at 4.7 T, while those of *in vivo* human fat at 1.9 T were within 500 ms or longer[18)] in rat at 2.0 T, except for the carbonyl carbons (1.94 s).[19)] Based on the T1 of glycogen in these reports, we chose TR of 500 ms in this study. Further optimization of TR for glycogen monitoring should be conducted using an *in vivo* model.

Another factor to reduce fat suppression is chemical shift displacement (CSD) of off-resonance signals induced by the field gradient in SAT. The signals of the metabolites contained in an organ are partially displaced into the volume selected for SAT, while some of those in the volume escape irradiation. This CSD problem is potentially not negligible, especially in ^{13}C MRS, since the chemical shift range (approximately 220 ppm) is wide, while that of protons is 10 ppm. A practical method to minimize the CSD is to set the center frequency of SAT on the chemical shift of the most interest. In this study, the CSD of glucose $^{13}C1\beta$ (96 ppm) was 1.9 mm with a field gradient strength of 2.21 gauss/cm, which was less than the gap (4.0 mm) among the components (Fig. 1), suggesting that the glucose signal was not strongly suppressed by the SAT pulse.

This CSD depends on the slice thickness of SAT. In order to avoid a significant effect of CSD, slice (slab) thickness of SAT should be optimized depending not only on the extent of CSD of the target signals but also on the anatomical (spatial) distance between the visceral fat and the tissue of interest obtained by the proton MR image. By arranging the gradient direction, the off-resonance signals of the metabolites can be shifted to the opposite side of the selected slice, leaving some signals out of the irradiated volume. When the peaks of interest are close to the lipid signals in frequency, the irradiation bandwidth of the CHESS pulses needs to be further optimized based on their excitation profile. Increasing the number of CHESS pulses, such as a triple CHESS pulse set frequently used in ^1H-MRS, will achieve more lipid signal suppression, however, it will not be an effective solution for ^{13}C-MRS, since it is difficult to safely cover the chemical shift range of lipid components widely distributed over the 200 ppm scale. Furthermore, it demands longer TR, resulting in a longer data acquisition time. Thus, we propose the combination pulse technique of a single CHESS pulse to suppress the main part of lipid peaks close to the glucose signal and a SAT pulse to spatially suppress the main part of fat tissue close to the surface coil.

One explanation for the discrepancy of the carbonyl signal reduction rate between the SAT pulse alone and the combination of SAT and CHESS pulses may be the pulse profile instability due to interference. The carbonyl carbon (168 ppm) of the oil is configured to be suppressed by the SAT pulse. The excitation profile in the frequency domain by the SAT pulse was close to rectanglular and its bandwidth was $\pm$3000 Hz with a center frequency of 82 ppm. The ^{13}C hard pulse to obtain ^{13}C FID signal has a *sinc* shaped profile with a bandwidth of $\pm$4000 Hz with the same center frequency. The carbonyl carbon was in the 2770 Hz lower field from the center frequency, and the location was near the

ends in both profiles. Since the methanol signal was within the suppression range of the CHESS pulse in the frequency domain, it was reasonable that most of the signal intensity was reduced (residual rate 13%). On the other hand, SAT pulse partially decreased the methanol signal (residual rate 87%), although the signal source was spatially out of the SAT suppression range. One possible explanation is spatial extension of the suppression profile by the side lobes, although it cannot be verified in this experiment design. The methanol component will not be the major factor in this contamination, since the CSD was calculated to be 4.5 mm and the inter-space between the components was 4.0 mm.

In conclusion, the potential advantage of combining two kinds of lipid suppression pulses for *in vivo* ^{13}C-MRS was demonstrated in this phantom study. As a future direction, the suppression profiles of the chemical shift domain by these two types of pulses should be further customized based on the *in vivo* ^{13}C peaks of interest. To achieve further improvements to extract the highest glucose peak (C1β) using this combined pulse method, the relaxation times in an *in vivo* environment, which are different from those *in vitro*, will be the main point to be considered.

References

1) Beckmann, N., Seelig, J. and Wick, H. (1990) Analysis of glycogen storage disease by *in vivo* ^{13}C NMR: comparison of normal volunteers with a patient. Magn. Reson. Med. **16**, 150–160.
2) Roser, W., Beckmann, N., Wiesmann, U. and Seelig, J. (1996) Absolute quantification of the hepatic glycogen content in a patient with glycogen storage disease by ^{13}C magnetic resonance spectroscopy. Magn. Reson. Imaging **14**, 1217–1220.
3) Fluck, C.E., Slotboom, J., Nuoffer, J.M., Kreis, R., Boesch, C. and Mullis, P.E. (2003) Normal hepatic glycogen storage after fasting and feeding in children and adolescents with type 1 diabetes. Pediatr. Diabetes **4**, 70–76.
4) Krssak, M., Brehm, A., Bernroider, E., Anderwald, C., Nowotny, P., Dalla Man, C., Cobelli, C., Cline, G.W., Shulman, G.I., Waldhäusl, W. and Roden, M. (2004) Alterations in postprandial hepatic glycogen metabolism in type 2 diabetes. Diabetes **53**, 3048–3056.
5) Ordidge, R.J., Connelly, A. and Lohman, J.A.B. (1986) Image-selected *in vivo* spectroscopy (ISIS). A new technique for spatially selective NMR spectroscopy. J. Magn. Reson. **66**, 283–294.
6) Doddrell, D.D., Galloway, G.J., Brooks, W.M., Bulsing, J.M., Field, J.C., Irving, M.G. and Baddeley, H. (1986) The utilization of two frequency-shifted sinc pulses for performing volume-selected *in vivo* NMR spectroscopy. Magn. Reson. Med. **3**, 970–975.
7) Choi, I.Y., Tkáč, I. and Gruetter, R. (2000) Single-shot, three-dimensional "non-echo" localization method for *in vivo* NMR spectroscopy. Magn. Reson. Med. **44**, 387–394.
8) Cunnane, S.C., Williams, S.C., Bell, J.D., Brookes, S., Craig, K., Iles, R.A. and Crawford, M.A. (1994) Utilization of uniformly labeled ^{13}C-polyunsaturated fatty acids in the synthesis of long-chain fatty acids and cholesterol accumulating in the neonatal rat brain. J. Neurochem. **62**, 2429–2436.
9) Haase, A., Frahm, J., Hänicke, W. and Mattaei, D. (1985) ^{1}H NMR chemical shift selective (CHESS) imaging. Phys. Med. Biol. **30**, 341–344.
10) Pauly, J.M., Le Roux, P., Nishimura, D.G. and Macovski, A. (1991) Parameter relations for the Shinnar–Le Roux selective excitation pulse design algorithm. IEEE Trans. Med. Imaging **10**, 53–65.
11) Ikonomidou, V.N. and Sergiadis, G.D. (2000) Improved Shinnar–Le Roux algorithm. J. Magn. Reson. **143**, 30–34.
12) Künnecke, B., Küstermann, E. and Seelig, J. (2000) Simultaneous *in vivo* monitoring of hepatic glucose and glucose-6-phosphate by ^{13}C-NMR spectroscopy. Magn. Reson. Med. **44**, 556–562.
13) Hwang, J.-H., Bluml, S., Leaf, A. and Ross, B.D. (2003) *In vivo* characterization of fatty acids in human adipose tissue using natural abundance ^{1}H decoupled ^{13}C MRS at 1.5 T: clinical applications to dietary therapy. NMR Biomed. **16**, 160–167.
14) Thomas, E.L., Frost, G., Barnard, M.L., Bryant, D.J., Taylor-Robinson, S.D., Simbrunner, J., Coutts, G.A., Burl, M., Bloom, S.R., Sales, K.D. and Bell, J.D. (1996) An *in vivo* ^{13}C magnetic resonance spectroscopic study of the relationship between diet and adipose tissue composition. Lipids **31**, 145–151.
15) Gottlieb, H.E., Kotlyar, V. and Nudelman, A. (1997) NMR chemical shifts of common laboratory solvents as trace impurities. J. Org. Chem. **62**, 7512–7515.
16) Zang, L.H., Laughlin, M.R., Rothman, D.L. and Shulman, R.G. (1990) Carbon-13 NMR relaxation times of hepatic glycogen *in vitro* and *in vivo*. Biochemistry **29**, 6815–6820.
17) Overloop, K., Vanstapel, F. and Van Hecke, P. (1996) ^{13}C-NMR relaxation in glycogen. Magn. Reson. Med. **36**, 45–51.
18) Fan, T.W.M., Clifford, A.J. and Higashi, R.M. (1994) *In vivo* ^{13}C NMR analysis of acyl chain composition and organization of perirenal triacylglycerides in rats fed vegetable and fish oils. J. Lipid Res. **35**, 678–689.
19) Moonen, C.T.W., Dimand, R.J. and Cox, K.L. (1988) The noninvasive determination of linoleic acid content of human adipose tissue by natural abundance carbon-13 nuclear magnetic resonance. Magn. Reson. Med. **6**, 140–157.

(Received Apr. 21, 2011; accepted June 2, 2011)